A Multiquantum State-To-State Model For The Fundamental States Of Air And Application To The Modeling Of High-Speed Shocked Flows

RHTGAE5, Barcelona, Spain, 16–19 October 2012

M. Lino da Silva, B. Lopez, V. Guerra, and J. Loureiro

Instituto de Plasmas e Fusão Nuclear
Instituto Superior Técnico, Lisboa, Portugal

16 October 2012

Objectives of the Presentation

General Objective: Presentation of a Complete State-Specific, Multiquantum, High-Temperature model for the ground states of N_2, O_2, and NO: The STELLAR database.

Outline of the Talk:

- Description of the Forced Harmonic Oscillator Method (FHO) for V–T, V–V–T, and V–D transitions modeling.
- Model capabilities for the prediction of high-temperature rates.
- Description of the rates database for the $N_2(X,v)$, $O_2(X,v)$, and NO(X,v) states. Aplication for a sample calculation (Fire II 0D calculation)

Objectives of the Presentation

General Objective: Presentation of a Complete State-Specific, Multiquantum, High-Temperature model for the ground states of N_2, O_2, and NO: The STELLAR database.

Outline of the Talk:

- Description of the Forced Harmonic Oscillator Method (FHO) for V–T, V–V–T, and V–D transitions modeling.
- Model capabilities for the prediction of high-temperature rates.
- Description of the rates database for the N_2(X,v), O_2(X,v), and NO(X,v) states. Aplication for a sample calculation (Fire II 0D calculation)

INSTITUTO SUPERIOR TÉCNICO

Objectives of the Presentation

General Objective: Presentation of a Complete State-Specific, Multiquantum, High-Temperature model for the ground states of N_2, O_2, and NO: The STELLAR database.

Outline of the Talk:

- Description of the Forced Harmonic Oscillator Method (FHO) for V–T, V–V–T, and V–D transitions modeling.
- Model capabilities for the prediction of high-temperature rates.
- Description of the rates database for the $N_2(X,v)$, $O_2(X,v)$, and NO(X,v) states. Aplication for a sample calculation (Fire II 0D calculation)

Objectives of the Presentation

General Objective: Presentation of a Complete State-Specific, Multiquantum, High-Temperature model for the ground states of N_2, O_2, and NO: The STELLAR database.

Outline of the Talk:

- Description of the Forced Harmonic Oscillator Method (FHO) for V–T, V–V–T, and V–D transitions modeling.
- Model capabilities for the prediction of high-temperature rates.
- Description of the rates database for the N_2(X,v), O_2(X,v), and NO(X,v) states. Aplication for a sample calculation (Fire II 0D calculation)

Objectives of the Presentation

General Objective: Presentation of a Complete State-Specific, Multiquantum, High-Temperature model for the ground states of N_2, O_2, and NO: The STELLAR database.

Outline of the Talk:

- Description of the Forced Harmonic Oscillator Method (FHO) for V–T, V–V–T, and V–D transitions modeling.
- Model capabilities for the prediction of high-temperature rates.
- Description of the rates database for the N_2(X,v), O_2(X,v), and NO(X,v) states. Aplication for a sample calculation (Fire II 0D calculation)

General Models for V–T, V–V–T and V–D Processes Simulation

- Progresses in Quantum chemistry have introduced increasingly accurate atom-diatom and diatom-diatom potentials.
- Trajectory methods over such potentials can provide very detailed state-specific data. But these methods revain very intensive for the systematic production of rate databases
- Over the last decades, FOPT methods (Such as the SSH approach) have been utilized, with a relative degree of success, for the modeling of heavy-impact processes in low-T plasmas

	FOPT (SSH)	FHO	Trajectory Methods
Collision Trajectories	1D repulsive /attractive	1D repulsive/attractive 3D repulsive	3D
Collison Energy	perturbative (only low T)	Any	Any
energy jumps	$\Delta E_{i \to j} > \Delta E_{tr}$	Any	Any
multiquantum	No	Yes	Yes
Transition Type	Non-Reactive	Non-Reactive	Non-Reactive & Reactive
Intermolecular Potential	Isotropic	Isotropic	Any

Respective characteristics of FOPT, FHO, and trajectory methods

- FHO model proposed at the same time than FOPT models (Rapp&Sharp:1963, Zelechow:1968), but only systematically deployed much later due to computational constraints (Adamovich:1995, LinodaSilva:2007).

An Accurate, Physically-Consistent, Semianalytic Model for the prediction of V–T, V–V–T and V–D Processes

- FHO model nicely reproduces results from more sophisticated approaches (QCT methods, etc...), and is physically consistent at high T.
- SSH model also nicely scales at low T, but fails at high T.
- For a large range of plasma sources, VT and VD processes can only be properly simulated through the FHO model or sophisticated methods.
- The FHO model provides an interesting bridging theory for the modeling of "contemporary" plasma sources.

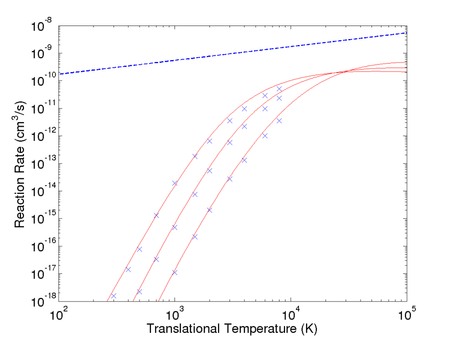

1→0, 9→8, and 20→19 N_2–N_2 V–T rates. Comparison between Billing's QCT rates (×) and the FHO model (–)

INSTITUTO SUPERIOR TÉCNICO

An Accurate, Physically-Consistent, Semianalytic Model for the prediction of V–T, V–V–T and V–D Processes

- FHO model nicely reproduces results from more sophisticated approaches (QCT methods, etc...), and is physically consistent at high T.
- SSH model also nicely scales at low T, but fails at high T.
- For a large range of plasma sources, VT and VD processes can only be properly simulated through the FHO model or sophisticated methods.

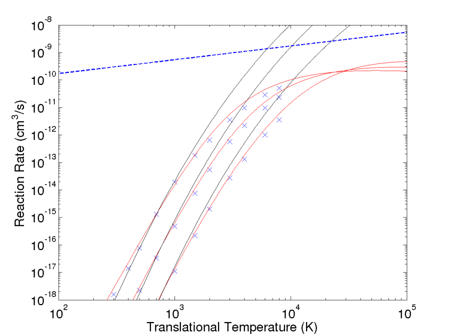

1→0, 9→8, and 20→19 N_2–N_2 V–T rates. Comparison between Billing's QCT rates (×) and the FHO model (–). SSH rates are added

- The FHO model provides an interesting bridging theory for the modeling of “contemporary” plasma sources.

INSTITUTO SUPERIOR TÉCNICO

An Accurate, Physically-Consistent, Semianalytic Model for the prediction of V–T, V–V–T and V–D Processes

- FHO model nicely reproduces results from more sophisticated approaches (QCT methods, etc...), and is physically consistent at high T.
- SSH model also nicely scales at low T, but fails at high T.
- For a large range of plasma sources, VT and VD processes can only be properly simulated through the FHO model or sophisticated methods.

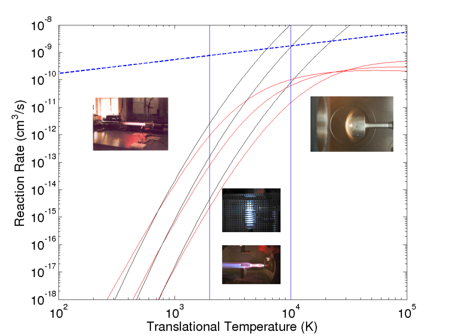

- The FHO model provides an interesting bridging theory for the modeling of "contemporary" plasma sources.

INSTITUTO SUPERIOR TÉCNICO

An Accurate, Physically-Consistent, Semianalytic Model for the prediction of V–T, V–V–T and V–D Processes

- FHO model nicely reproduces results from more sophisticated approaches (QCT methods, etc...), and is physically consistent at high T.
- SSH model also nicely scales at low T, but fails at high T.
- For a large range of plasma sources, VT and VD processes can only be properly simulated through the FHO model or sophisticated methods.

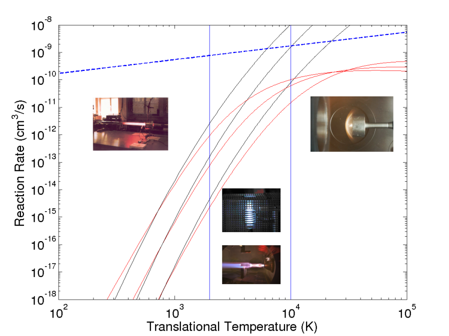

- The FHO model provides an interesting bridging theory for the modeling of "contemporary" plasma sources.

The Forced Harmonic Oscillator Model in 2 Slides

– V–T transition probabilities for collinear atom-diatom non-reactive collisions are given by Kerner and Treanor

$$P(i \to f, \varepsilon) = i!f!\varepsilon^{i+f} \exp(-\varepsilon) \left| \sum_{r=0}^{n} \frac{(-1)^r}{r!(i-r)!(f-r)!\varepsilon^r} \right|^2$$

with $n = min(i, f)$.

– V–V–T transition probabilities for collinear diatom-diatom collisions are given[1] by Zelechow

$$P(i_1, i_2 \to f_1, f_2, \varepsilon, \rho) = \left| \sum_{g=1}^{n} (-1)^{(i_{12}-g+1)} C^{i_{12}}_{g,i_2+1} C^{f_{12}}_{g,f_2+1} \varepsilon^{\frac{1}{2}(i_{12}+f_{12}-2g+2)} \exp(-\varepsilon/2) \right.$$
$$\left. \times \sqrt{(i_{12}-g+1)!(f_{12}-g+1)!} \exp[-i(f_{12}-g+1)\rho] \sum_{l=0}^{n-g} \frac{(-1)^l}{(i_{12}-g+1-l)!(f_{12}-g+1-l)!l!\varepsilon^l} \right|^2$$

with $i_{12} = i_1 + i_2$, $f_{12} = f_1 + f_2$ and $n = min(i_1 + i_2 + 1, f_1 + f_2 + 1)$.

In these equations ε and ρ are related to the two-state FOPT transition probabilities, with $\varepsilon = P_{\mathrm{FOPT}}(1 \to 0)$ and $\rho = [4 \cdot P_{\mathrm{FOPT}}(1, 0 \to 0, 1)]^{1/2}$.

C^k_{ij} is a transformation matrix calculated according to the expression[1]

$$C^k_{ij} = 2^{-n/2} \binom{k}{i-1}^{-1/2} \binom{k}{j-1}^{1/2} \times \sum_{v=0}^{j-1} (-1)^v \binom{k-i+1}{j-v-1} \binom{i-1}{v}.$$

INSTITUTO SUPERIOR TÉCNICO

[1] Corrected from typographic errors

The Forced Harmonic Oscillator Model in 2 Slides

– V–T transition probabilities for collinear atom-diatom non-reactive collisions are given by Kerner and Treanor

$$P(i \to f, \varepsilon) = i!f!\varepsilon^{i+f} \exp(-\varepsilon) \left| \sum_{r=0}^{n} \frac{(-1)^r}{r!(i-r)!(f-r)!\varepsilon^r} \right|^2$$

with $n = min(i, f)$.

– V–V–T transition probabilities for collinear diatom-diatom collisions are given[1] by Zelechow

$$P(i_1, i_2 \to f_1, f_2, \varepsilon, \rho) = \left| \sum_{g=1}^{n} (-1)^{(i_{12}-g+1)} C^{i_{12}}_{g,i_2+1} C^{f_{12}}_{g,f_2+1} \varepsilon^{\frac{1}{2}(i_{12}+f_{12}-2g+2)} \exp(-\varepsilon/2) \right.$$

$$\left. \times \sqrt{(i_{12}-g+1)!(f_{12}-g+1)!} \exp[-i(f_{12}-g+1)\rho] \sum_{l=0}^{n-g} \frac{(-1)^l}{(i_{12}-g+1-l)!(f_{12}-g+1-l)!l!\varepsilon^l} \right|^2$$

with $i_{12} = i_1 + i_2$, $f_{12} = f_1 + f_2$ and $n = min(i_1 + i_2 + 1, f_1 + f_2 + 1)$.

In these equations ε and ρ are related to the two-state FOPT transition probabilities, with $\varepsilon = P_{\mathrm{FOPT}}(1 \to 0)$ and $\rho = [4 \cdot P_{\mathrm{FOPT}}(1, 0 \to 0, 1)]^{1/2}$.

C^k_{ij} is a transformation matrix calculated according to the expression[1]

$$C^k_{ij} = 2^{-n/2} \binom{k}{i-1}^{-1/2} \binom{k}{j-1}^{1/2} \times \sum_{v=0}^{j-1} (-1)^v \binom{k-i+1}{j-v-1} \binom{i-1}{v}.$$

[1] Corrected from typographic errors

The Forced Harmonic Oscillator Model in 2 Slides

– V–T transition probabilities for collinear atom-diatom non-reactive collisions are given by Kerner and Treanor

$$P(i \rightarrow f, \varepsilon) = i!f!\varepsilon^{i+f} \exp(-\varepsilon) \left| \sum_{r=0}^{n} \frac{(-1)^r}{r!(i-r)!(f-r)!\varepsilon^r} \right|^2$$

with $n = min(i, f)$.

– V–V–T transition probabilities for collinear diatom-diatom collisions are given[1] by Zelechow

$$P(i_1, i_2 \rightarrow f_1, f_2, \varepsilon, \rho) = \left| \sum_{g=1}^{n} (-1)^{(i_{12}-g+1)} C^{i_{12}}_{g,i_2+1} C^{f_{12}}_{g,f_2+1} \varepsilon^{\frac{1}{2}(i_{12}+f_{12}-2g+2)} \exp(-\varepsilon/2) \right.$$

$$\left. \times \sqrt{(i_{12}-g+1)!(f_{12}-g+1)!} \exp[-i(f_{12}-g+1)\rho] \sum_{l=0}^{n-g} \frac{(-1)^l}{(i_{12}-g+1-l)!(f_{12}-g+1-l)!l!\varepsilon^l} \right|^2$$

with $i_{12} = i_1 + i_2$, $f_{12} = f_1 + f_2$ and $n = min(i_1 + i_2 + 1, f_1 + f_2 + 1)$.

In these equations ε and ρ are related to the two-state FOPT transition probabilities, with $\varepsilon = P_{\mathrm{FOPT}}(1 \rightarrow 0)$ and $\rho = [4 \cdot P_{\mathrm{FOPT}}(1,0 \rightarrow 0,1)]^{1/2}$.

C^k_{ij} is a transformation matrix calculated according to the expression[1]

$$C^k_{ij} = 2^{-n/2} \binom{k}{i-1}^{-1/2} \binom{k}{j-1}^{1/2} \times \sum_{v=0}^{j-1} (-1)^v \binom{k-i+1}{j-v-1} \binom{i-1}{v}.$$

[1] Corrected from typographic errors

The Forced Harmonic Oscillator Model in 2 Slides

For a purely repulsive intermolecular potential $V(r) \sim \exp(-\alpha r)$, expressions for ε and ρ are given by Zelechow

$$\varepsilon = \frac{8\pi^3\omega\left(\tilde{m}^2/\mu\right)\gamma^2}{\alpha^2 h}\sinh^{-2}\left(\frac{\pi\omega}{\alpha\bar{v}}\right), \qquad \rho = 2\left(\tilde{m}^2/\mu\right)\gamma^2\alpha\bar{v}/\omega.$$

For a Morse intermolecular potential $V(r) \sim E_m(1-\exp(-\alpha r))^2$, the expression for ε is given by Cottrell (the expression for ρ remains identical)

$$\varepsilon = \frac{8\pi^3\omega\left(\tilde{m}^2/\mu\right)\gamma^2}{\alpha^2 h}\frac{\cosh^2\left[\frac{(1+\phi)\pi\omega}{\alpha\bar{v}}\right]}{\sinh^2\left(\frac{2\pi\omega}{\alpha\bar{v}}\right)}, \qquad \phi = (2/\pi)\tan^{-1}\sqrt{\left(2E_m/\tilde{m}\bar{v}^2\right)}.$$

E_m represents the potential well, ω denotes the oscillator frequency, and μ, γ, and $\tilde{m}$ are mass parameters

Adamovich and Macheret summarized and introduced a few improvements for generalizing the FHO theory for arbitrary molecular collisions:

- symmetrization of the collision velocity to enforce detailed balance (median collision velocity $\bar{v} = (v_i + v_f)/2$);
- accounting for the anharmonicity of the oscillator potential curve using an average frequency $\omega = |(E_i - E_f)/(i-f)|$ if $i \neq f$, and $\omega = \left|E_{i+1} - E_i\right|$ if $i = f$;
- Generalization of the model for nonresonant V–V–T transitions and V–V–T transitions between different species, by replacing $\rho \to \rho \times \xi/\sinh(\xi)$, with $\xi = \pi^2(\omega_1 - \omega_2)/4\alpha\bar{v}$;
- Generalization of the FHO model to non-collinear collisions (general case) through the multiplication of the parameters ϵ and ρ by steric factors such that $\varepsilon = \varepsilon \times S_{VT}$ and $\rho = \rho \times \sqrt{S_{VV}}$, using the values $S_{VT} = 4/9$ and $S_{VV} = 1/27$, as proposed by Adamovich

INSTITUTO SUPERIOR TÉCNICO

The Forced Harmonic Oscillator Model in 2 Slides

For a purely repulsive intermolecular potential $V(r) \sim \exp(-\alpha r)$, expressions for ε and ρ are given by Zelechow

$$\varepsilon = \frac{8\pi^3\omega\left(\tilde{m}^2/\mu\right)\gamma^2}{\alpha^2 h}\sinh^{-2}\left(\frac{\pi\omega}{\alpha\bar{v}}\right), \qquad \rho = 2\left(\tilde{m}^2/\mu\right)\gamma^2\alpha\bar{v}/\omega.$$

For a Morse intermolecular potential $V(r) \sim E_m(1-\exp(-\alpha r))^2$, the expression for ε is given by Cottrell (the expression for ρ remains identical)

$$\varepsilon = \frac{8\pi^3\omega\left(\tilde{m}^2/\mu\right)\gamma^2}{\alpha^2 h}\frac{\cosh^2\left[\frac{(1+\phi)\pi\omega}{\alpha\bar{v}}\right]}{\sinh^2\left(\frac{2\pi\omega}{\alpha\bar{v}}\right)}, \qquad \phi = (2/\pi)\tan^{-1}\sqrt{(2E_m/\tilde{m}\bar{v}^2)}.$$

E_m represents the potential well, ω denotes the oscillator frequency, and μ, γ, and $\tilde{m}$ are mass parameters

Adamovich and Macheret summarized and introduced a few improvements for generalizing the FHO theory for arbitrary molecular collisions:

- symmetrization of the collision velocity to enforce detailed balance (median collision velocity $\bar{v} = (v_i + v_f)/2$);
- accounting for the anharmonicity of the oscillator potential curve using an average frequency $\omega = |(E_i - E_f)/(i-f)|$ if $i \neq f$, and $\omega = |E_{i+1} - E_i|$ if $i = f$;
- Generalization of the model for nonresonant V–V–T transitions and V–V–T transitions between different species, by replacing $\rho \to \rho \times \xi/\sinh(\xi)$, with $\xi = \pi^2(\omega_1 - \omega_2)/4\alpha\bar{v}$;
- Generalization of the FHO model to non-collinear collisions (general case) through the multiplication of the parameters ϵ and ρ by steric factors such that $\varepsilon = \varepsilon \times S_{VT}$ and $\rho = \rho \times \sqrt{S_{VV}}$, using the values $S_{VT} = 4/9$ and $S_{VV} = 1/27$, as proposed by Adamovich

The Forced Harmonic Oscillator Model in 2 Slides

For a purely repulsive intermolecular potential $V(r) \sim \exp(-\alpha r)$, expressions for ε and ρ are given by Zelechow

$$\varepsilon = \frac{8\pi^3\omega\left(\tilde{m}^2/\mu\right)\gamma^2}{\alpha^2 h}\sinh^{-2}\left(\frac{\pi\omega}{\alpha\bar{v}}\right), \qquad \rho = 2\left(\tilde{m}^2/\mu\right)\gamma^2\alpha\bar{v}/\omega.$$

For a Morse intermolecular potential $V(r) \sim E_m(1-\exp(-\alpha r))^2$, the expression for ε is given by Cottrell (the expression for ρ remains identical)

$$\varepsilon = \frac{8\pi^3\omega\left(\tilde{m}^2/\mu\right)\gamma^2}{\alpha^2 h}\frac{\cosh^2\left[\frac{(1+\phi)\pi\omega}{\alpha\bar{v}}\right]}{\sinh^2\left(\frac{2\pi\omega}{\alpha\bar{v}}\right)}, \qquad \phi = (2/\pi)\tan^{-1}\sqrt{(2E_m/\tilde{m}\bar{v}^2)}.$$

E_m represents the potential well, ω denotes the oscillator frequency, and μ, γ, and $\tilde{m}$ are mass parameters

Adamovich and Macheret summarized and introduced a few improvements for generalizing the FHO theory for arbitrary molecular collisions:

- symmetrization of the collision velocity to enforce detailed balance (median collision velocity $\bar{v} = (v_i + v_f)/2$);
- accounting for the anharmonicity of the oscillator potential curve using an average frequency $\omega = |(E_i - E_f)/(i-f)|$ if $i \neq f$, and $\omega = |E_{i+1} - E_i|$ if $i = f$;
- Generalization of the model for nonresonant V–V–T transitions and V–V–T transitions between different species, by replacing $\rho \rightarrow \rho \times \xi/\sinh(\xi)$, with $\xi = \pi^2(\omega_1 - \omega_2)/4\alpha\bar{v}$;
- Generalization of the FHO model to non-collinear collisions (general case) through the multiplication of the parameters ϵ and ρ by steric factors such that $\varepsilon = \varepsilon \times S_{VT}$ and $\rho = \rho \times \sqrt{S_{VV}}$, using the values $S_{VT} = 4/9$ and $S_{VV} = 1/27$, as proposed by Adamovich

INSTITUTO SUPERIOR TÉCNICO

The Forced Harmonic Oscillator Model in 2 Slides

For a purely repulsive intermolecular potential $V(r) \sim \exp(-\alpha r)$, expressions for ε and ρ are given by Zelechow

$$\varepsilon = \frac{8\pi^3\omega\left(\tilde{m}^2/\mu\right)\gamma^2}{\alpha^2 h}\sinh^{-2}\left(\frac{\pi\omega}{\alpha\bar{v}}\right), \qquad \rho = 2\left(\tilde{m}^2/\mu\right)\gamma^2\alpha\bar{v}/\omega.$$

For a Morse intermolecular potential $V(r) \sim E_m(1-\exp(-\alpha r))^2$, the expression for ε is given by Cottrell (the expression for ρ remains identical)

$$\varepsilon = \frac{8\pi^3\omega\left(\tilde{m}^2/\mu\right)\gamma^2}{\alpha^2 h}\frac{\cosh^2\left[\frac{(1+\phi)\pi\omega}{\alpha\bar{v}}\right]}{\sinh^2\left(\frac{2\pi\omega}{\alpha\bar{v}}\right)}, \qquad \phi = (2/\pi)\tan^{-1}\sqrt{(2E_m/\tilde{m}\bar{v}^2)}.$$

E_m represents the potential well, ω denotes the oscillator frequency, and μ, γ, and $\tilde{m}$ are mass parameters

Adamovich and Macheret summarized and introduced a few improvements for generalizing the FHO theory for arbitrary molecular collisions:

- symmetrization of the collision velocity to enforce detailed balance (median collision velocity $\bar{v} = (v_i + v_f)/2$);
- accounting for the anharmonicity of the oscillator potential curve using an average frequency $\omega = |(E_i - E_f)/(i-f)|$ if $i \neq f$, and $\omega = \left|E_{i+1} - E_i\right|$ if $i = f$;
- Generalization of the model for nonresonant V–V–T transitions and V–V–T transitions between different species, by replacing $\rho \to \rho \times \xi/\sinh(\xi)$, with $\xi = \pi^2(\omega_1 - \omega_2)/4\alpha\bar{v}$;
- Generalization of the FHO model to non-collinear collisions (general case) through the multiplication of the parameters ϵ and ρ by steric factors such that $\varepsilon = \varepsilon \times S_{VT}$ and $\rho = \rho \times \sqrt{S_{VV}}$, using the values $S_{VT} = 4/9$ and $S_{VV} = 1/27$, as proposed by Adamovich

Some Further Assumptions (Extra Slide 3)

At high T, multiquantum V–V–T transitions have to be accounted for. This is impractical as the number of transitions becomes N^4 where N is the number of vibrational levels (ex. N=61 for N_2).
Adamovich verified that for $E_{tr} \gg E_{vib}$, V–V–T processes occur as two independent V–T processes, and pure V–V exchanges can be neglected (roughly for $T > 10,000\mathrm{K}$). We then have:

$$P_{VVT}(i_1, i_2 \to f_1, f_2, \varepsilon, \rho) \cong P_{VT}(i_1 \to f_1, \varepsilon) \cdot P_{VT}(i_2 \to f_2, \varepsilon)$$
$$P_{VT}(i_1, \mathrm{all} \to f_1, \mathrm{all}, \varepsilon, \rho) = P_{VT}(i_1 \to f_1, \varepsilon)$$

which leads to a more practical calculation of N^2 rates.

V–D processes such as $AB(i) + M \rightleftarrows A + B + M$ are modeled according to the approach proposed by Macheret and Adamovich. The probability for dissociation as the product of the transition probability to a quasi-bound state such that $v > v_{diss}$, times the probability of the subsequent decay of the energetic complex

$$P(i \to, \varepsilon) = P(i \to v_{qbound}, \varepsilon) \cdot P_{decay} \quad (1)$$

with $P_{decay} \sim 1$.

Numerical Implementation of the FHO Model

Factorials in denominators/numerators of probabilities expressions lead to overflows/underflows for high quantum numbers

Factorial→Bessel

$$P(i \to f, \varepsilon) = J_s^2\left(2\sqrt{n_s \varepsilon}\right)$$

for $i, f \gg s = |i - f|$, and $n_s = [max(i, f)!min(i, f)!]^{-s}$, and

$$P(i_1, i_2 \to f_1, f_2, \varepsilon, \rho) = J_s^2\left[2\left(n_s^{(1)} n_s^{(2)} \rho_\xi^2/4\right)^{1/2}\right]$$

for $i_1 + i_2 = f_1 + f_2$, and $i_1 + i_2 + f_1 + f_2 \gg s = |i_1 - f_1|$.

Bessel→Polynom

$$J_s^2\left(2\sqrt{n_s \varepsilon}\right) \simeq \frac{(n_s)^s}{(s!)^2} \varepsilon^s \exp\left(\frac{-2 n_s \varepsilon}{s+1}\right);$$

$$J_s^2\left[2\left(n_s^{(1)} n_s^{(2)} \rho_\xi^2/4\right)^{1/2}\right] \simeq \frac{\left[n_s^{(1)} n_s^{(2)}\right]^s}{(s!)^2} \left(\frac{\rho_\xi^2}{4}\right)^s \exp\left(-\frac{n_s^{(1)} n_s^{(2)}}{s+1} \frac{\rho_\xi^2}{4}\right)$$

Numerical Implementation of the FHO Model

Factorials in denominators/numerators of probabilities expressions lead to overflows/underflows for high quantum numbers

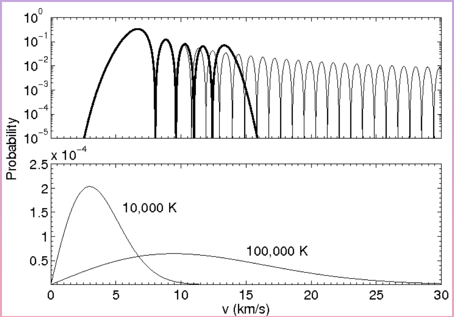

Exact (bold) and asymptotic probability (light) for a 5 → 4 N_2–N_2 V–T collision (upper figure) and maxwellian velocity distribution functions at 10,000 K and 100,000 K (lower figure)

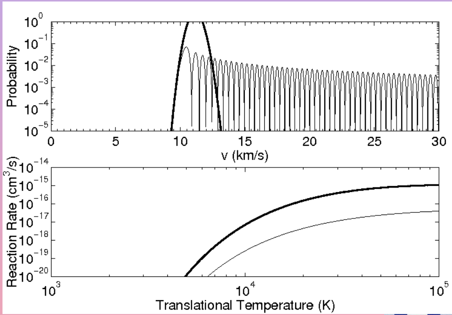

Nikitin (light) and Exact (bold) asymptotic transition probabilities for a 15 → 30 N_2–N_2 V–T collision as a function of the colliding velocity (upper figure) and corresponding reaction rates against the translational temperature (lower figure).

INSTITUTO SUPERIOR TÉCNICO

Numerical Implementation of the FHO Model

Factorials in denominators/numerators of probabilities expressions lead to overflows/underflows for high quantum numbers

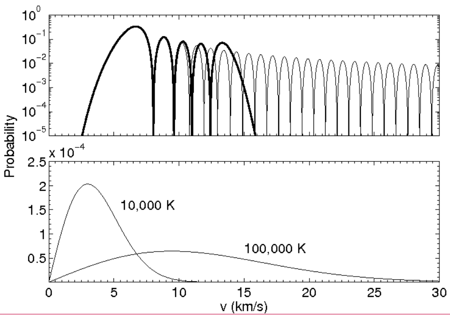

Exact (bold) and asymptotic probability (light) for a 5 → 4 N_2–N_2 V–T collision (upper figure) and maxwellian velocity distribution functions at 10,000 K and 100,000 K (lower figure)

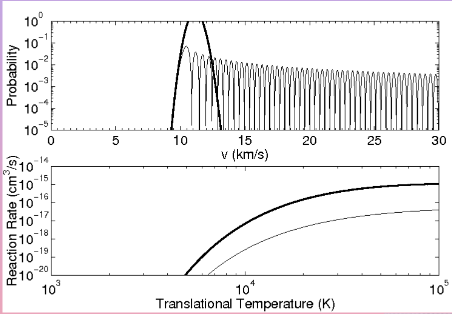

Nikitin (light) and Exact (bold) asymptotic transition probabilities for a 15 → 30 N_2–N_2 V–T collision as a function of the colliding velocity (upper figure) and corresponding reaction rates against the translational temperature (lower figure).

Only the Bessel approximation can be recommended for low-intermediate temperatures

The Question of Accurate Level Energies Calculations

- Typical level energies calculations rely on polynomial expansions. These are not accurate outside their initial fit range.
- Potential reconstruction methods (+ solving the radial Schrödinger equation) allow accurate extrapolations up to the dissociation energy.
- For $N_2(X)$, a RKR method and a more sophisticated DPF method both yield v_{max}=60 instead of the traditional v_{max}=45-47. The 2D limit of the Lagana N_3 potential considered by the Bari team yields v_{max}=67.

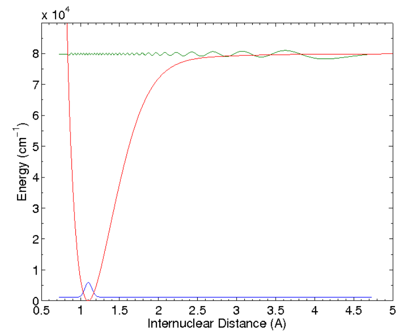

- Inaccurate level energies lead to orders of magnitude differences (N_2 dissociation rates; Pink Afterglow times. (see LinodaSilva, PSST 2009 & LinodaSilva, ChemPhys 2008)

INSTITUTO SUPERIOR TÉCNICO

The Question of Accurate Level Energies Calculations

- Typical level energies calculations rely on polynomial expansions. These are not accurate outside their initial fit range.
- Potential reconstruction methods (+ solving the radial Schrödinger equation) allow accurate extrapolations up to the dissociation energy.
- For $N_2(X)$, a RKR method and a more sophisticated DPF method both yield v_{max}=60 instead of the traditional v_{max}=45-47. The 2D limit of the Lagana N_3 potential considered by the Bari team yields v_{max}=67.

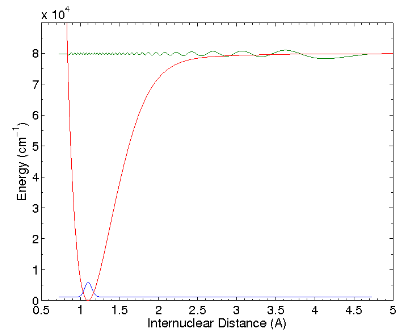

- Inaccurate level energies lead to orders of magnitude differences (N_2 dissociation rates; Pink Afterglow times. (see LinodaSilva, PSST 2009 & LinodaSilva, ChemPhys 2008)

INSTITUTO SUPERIOR TÉCNICO

The Question of Accurate Level Energies Calculations

- Typical level energies calculations rely on polynomial expansions. These are not accurate outside their initial fit range.
- Potential reconstruction methods (+ solving the radial Schrödinger equation) allow accurate extrapolations up to the dissociation energy.
- For $N_2(X)$, a RKR method and a more sophisticated DPF method both yield v_{max}=60 instead of the traditional v_{max}=45-47. The 2D limit of the Lagana N_3 potential considered by the Bari team yields v_{max}=67.

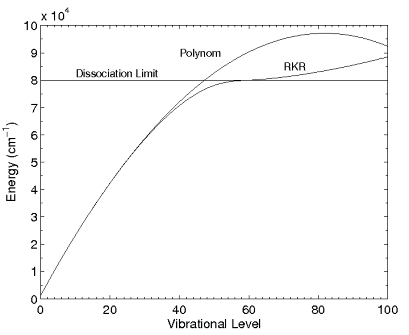

- Inaccurate level energies lead to orders of magnitude differences (N_2 dissociation rates; Pink Afterglow times. (see LinodaSilva, PSST 2009 & LinodaSilva, ChemPhys 2008)

INSTITUTO SUPERIOR TÉCNICO

The Question of Accurate Level Energies Calculations

- Typical level energies calculations rely on polynomial expansions. These are not accurate outside their initial fit range.
- Potential reconstruction methods (+ solving the radial Schrödinger equation) allow accurate extrapolations up to the dissociation energy.
- For $N_2(X)$, a RKR method and a more sophisticated DPF method both yield v_{max}=60 instead of the traditional v_{max}=45-47. The 2D limit of the Lagana N_3 potential considered by the Bari team yields v_{max}=67.

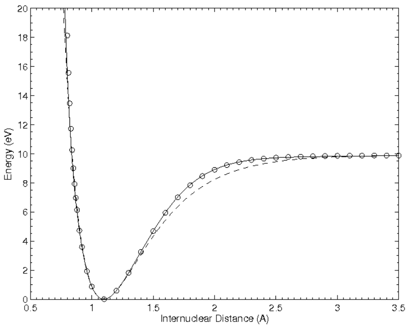

- Inaccurate level energies lead to orders of magnitude differences (N_2 dissociation rates; Pink Afterglow times. (see LinodaSilva, PSST 2009 & LinodaSilva, ChemPhys 2008)

The Question of Accurate Level Energies Calculations

- Typical level energies calculations rely on polynomial expansions. These are not accurate outside their initial fit range.
- Potential reconstruction methods (+ solving the radial Schrödinger equation) allow accurate extrapolations up to the dissociation energy.
- For $N_2(X)$, a RKR method and a more sophisticated DPF method both yield v_{max}=60 instead of the traditional v_{max}=45-47. The 2D limit of the Lagana N_3 potential considered by the Bari team yields v_{max}=67.

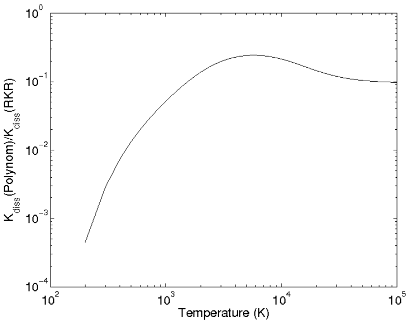

- Inaccurate level energies lead to orders of magnitude differences (N_2 dissociation rates; Pink Afterglow times. (see LinodaSilva, PSST 2009 & LinodaSilva, ChemPhys 2008)

The Question of Accurate Level Energies Calculations

- Typical level energies calculations rely on polynomial expansions. These are not accurate outside their initial fit range.
- Potential reconstruction methods (+ solving the radial Schrödinger equation) allow accurate extrapolations up to the dissociation energy.
- For $N_2(X)$, a RKR method and a more sophisticated DPF method both yield $v_{max}=60$ instead of the traditional $v_{max}=45$-47. The 2D limit of the Lagana N_3 potential considered by the Bari team yields $v_{max}=67$.

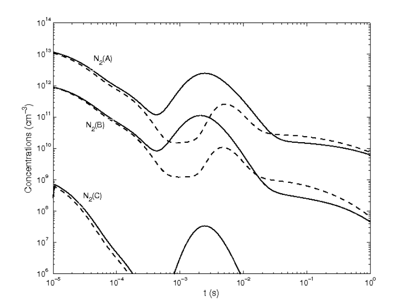

- Inaccurate level energies lead to orders of magnitude differences (N_2 dissociation rates; Pink Afterglow times. (see LinodaSilva, PSST 2009 & LinodaSilva, ChemPhys 2008)

Development of Detailed Databases for Multiquantum V–T and V–D transitions in Air

- We compiled the existing multiquantum state-specific datasets for Air (Esposito, Atom-Diatom collisions; Bose, Zeldovich reactions). These reactions have been reinterpolated to an accurate list of vibrational levels obtained through potential reconstruction methods.
- The remainder missing rates have been produced by our group for diatom-diatom collisions, to the largest accuracy possible with the FHO model (using the exact factorial expressions).

INSTITUTO SUPERIOR TÉCNICO

Development of Detailed Databases for Multiquantum V–T and V–D transitions in Air

- We compiled the existing multiquantum state-specific datasets for Air (Esposito, Atom-Diatom collisions; Bose, Zeldovich reactions). These reactions have been reinterpolated to an accurate list of vibrational levels obtained through potential reconstruction methods.
- The remainder missing rates have been produced by our group for diatom-diatom collisions, to the largest accuracy possible with the FHO model (using the exact factorial expressions).

INSTITUTO SUPERIOR TÉCNICO

Development of Detailed Databases for Multiquantum V–T and V–D transitions in Air

No.	Reaction	Model	α^{-1} (Å)	E (K)	N	Ref.
1	$N_2(X,v_i) + N_2 \rightleftarrows N_2(X,v_f) + N_2$	FHO	4	200	3721	LinodaSilva:2010
2	$N_2(X,v_i) + N_2 \rightleftarrows N + N + N_2$	FHO	4	200	124	LinodaSilva:2010
3	$N_2(X,v_i) + O_2 \rightleftarrows N_2(X,v_f) + O_2$	FHO	4	200	3721	LinodaSilva:2011
4	$N_2(X,v_i) + O_2 \rightleftarrows N + N + O_2$	FHO	4	200	124	LinodaSilva:2011
5	$O_2(X,v_i) + N_2 \rightleftarrows O_2(X,v_f) + N_2$	FHO	4	200	2116	LinodaSilva:2011
6	$O_2(X,v_i) + N_2 \rightleftarrows O + O + N_2$	FHO	4	200	92	LinodaSilva:2011
7	$O_2(X,v_i) + O_2 \rightleftarrows O_2(X,v_f) + O_2$	FHO	4	380	2116	LinodaSilva:2012
8	$O_2(X,v_i) + O_2 \rightleftarrows O + O + O_2$	FHO	4	380	92	LinodaSilva:2012
9	$N_2(X,v_i) + N \rightleftarrows N_2(X,v_f) + N$	QCT	–	–	3721	Esposito:2006
10	$N_2(X,v_i) + N \rightleftarrows N + N + N$	QCT	–	–	124	Esposito:2006
11	$O_2(X,v_i) + O \rightleftarrows O_2(X,v_f) + O$	QCT	–	–	2116	Esposito:2008
12	$O_2(X,v_i) + O \rightleftarrows O + O + O$	QCT	–	–	92	Esposito:2008
13	$N_2(X,v_i) + O \rightleftarrows N_2(X,v_f) + O$	FHO*	–	–	3721	Bose:1996
14	$N_2(X,v_i) + O \rightleftarrows N + N + O$	FHO*	–	–	124	Bose:1996
15	$O_2(X,v_i) + N \rightleftarrows O_2(X,v_f) + N$	FHO*	–	–	2116	Bose:1996
16	$O_2(X,v_i) + N \rightleftarrows O + O + N$	FHO*	–	–	92	Bose:1996
17	$N_2(X,v_i) + O \rightleftarrows NO(X,v_f) + N$	QCT	–	–	2928	Bose:1996
18	$O_2(X,v_i) + N \rightleftarrows NO(X,v_f) + O$	QCT	–	–	2208	Bose:1996
19	$NO(X,v_i) + N_2 \rightleftarrows NO(X,v_f) + N_2$	FHO	2	200	2304	LinodaSilva:2012
20	$NO(X,v_i) + N_2 \rightleftarrows N + O + N_2$	FHO	2	200	96	LinodaSilva:2012
21	$NO(X,v_i) + O_2 \rightleftarrows NO(X,v_f) + O_2$	FHO	2	380	2304	LinodaSilva:2012
22	$NO(X,v_i) + O_2 \rightleftarrows N + O + O_2$	FHO	2	380	96	LinodaSilva:2012

These 34148 Rates are compiled in the IST STELLAR 1.0 Database (available at http://esther.ist.utl.pt)

INSTITUTO SUPERIOR TÉCNICO

Database for N_2–N_2 Transitions

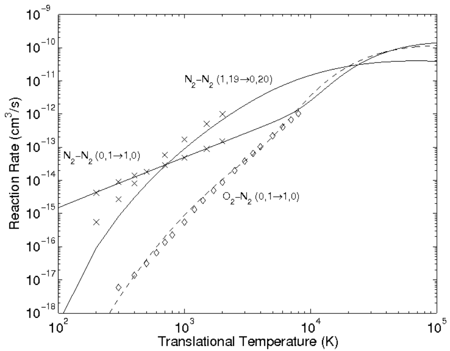

Single-quantum V–V rates for N_2–N_2 (0, 1→1, 0) and (0, 1→20, 19) transitions and O_2–N_2 (0, 1→1, 0) transitions. — and — —, FHO model. ×, calculations of Billing for N_2–N_2. ◇, interpolation of experimental data for N_2–O_2 (1, 0→0, 1), Taylor:1969.

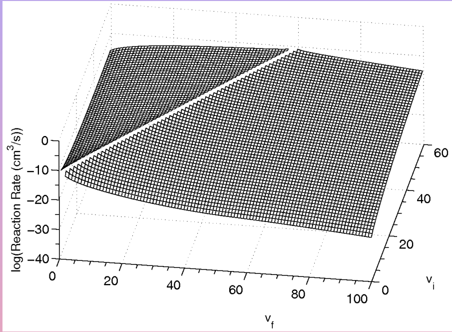

V–T Reaction rates at 10,000K. v_i and v_f denote the initial and final v–th level in the transition.

M. Lino da Silva, V. Guerra, and J. Loureiro, *J. Thermophys. Heat Transf.*, 2007.

INSTITUTO SUPERIOR TÉCNICO

Database for O_2–O_2 Transitions

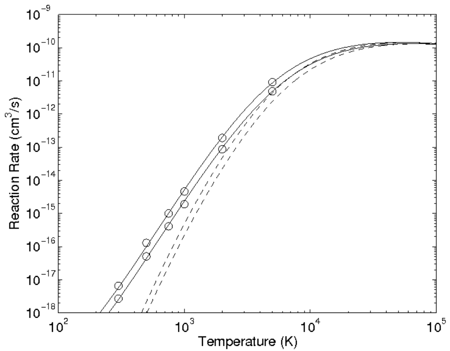

Single-quantum V–T rates for 1→0 and 2→1 transitions (bottom to top). —, FHO model ($E = 380$K); – –, FHO model (repulsive potential); o, calculations of Coletti and Billing.

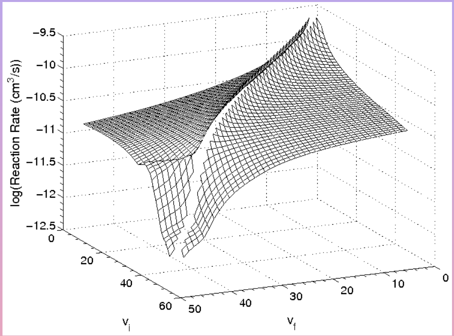

V–T Reaction rates at 100,000K. v_i and v_f denote the initial and final v–th level in the transition.

M. Lino da Silva, V. Guerra, and J. Loureiro, *Chem. Phys. Lett.*, 2012.

Reproduction of Equilibrium Dissociation Rates

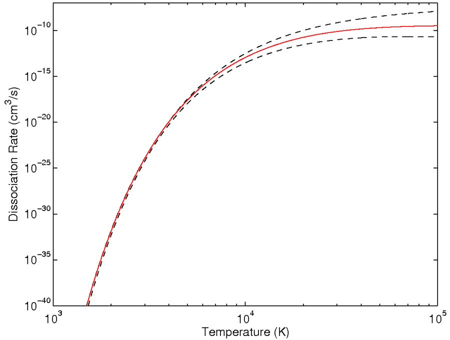

$N_2+N_2 \to N+N+N_2$ (LinodaSilva)

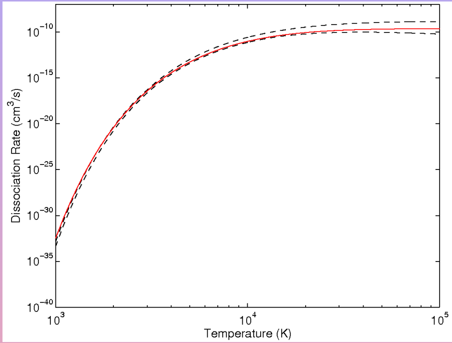

$O_2+O_2 \to O+O+O_2$ (LinodaSilva)

Comparison between FHO (red) and Macroscopic Kinetics Datasets

$$K_d^{eq} = Q_v(T) / \sum Q_v(T) k_d(v, T)$$

Excellent reproduction of equilibrium dissociation data.

Reproduction of Equilibrium Dissociation Rates

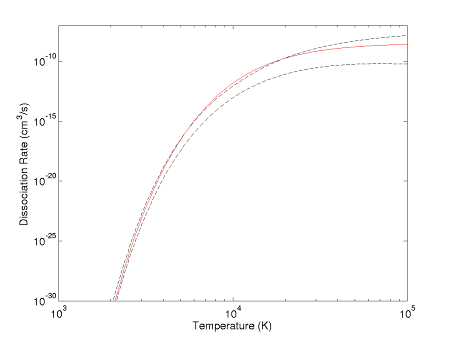

N_2+N→N+N+N (Esposito)

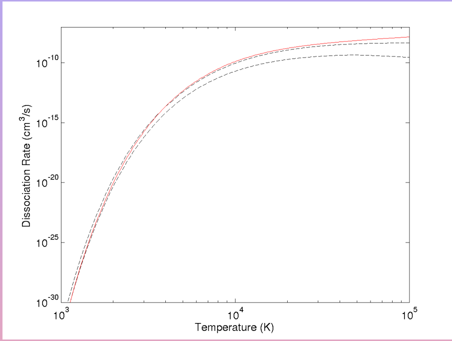

O_2+O→O+O+O (Esposito)

Comparison between FHO (red) and Macroscopic Kinetics Datasets

$$K_d^{eq} = Q_v(T) / \sum Q_v(T) k_d(v, T)$$

Excellent reproduction of equilibrium dissociation data.

Reproduction of Equilibrium Dissociation Rates

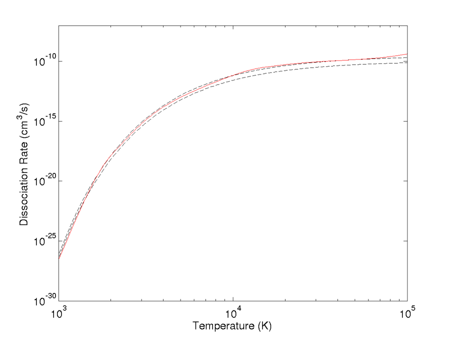

$N_2+O \rightarrow NO+N$ (Bose)

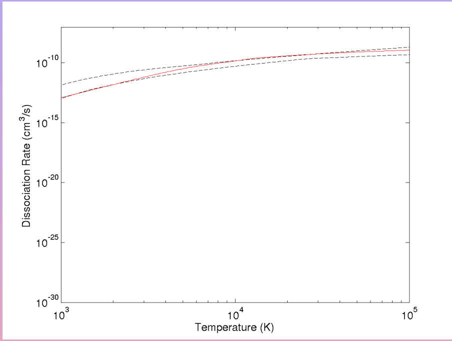

$O_2+N \rightarrow NO+O$ (Bose)

Comparison between FHO (red) and Macroscopic Kinetics Datasets

$$K_d^{eq} = Q_v(T) / \sum Q_v(T) k_d(v, T)$$

Excellent reproduction of equilibrium dissociation data.

Sample Applications and Future Work

Sample Applications

Towards an Adequate Accounting of Excited Levels and V–E Rates

- V–E tansitions presented as:
- $N_2(v) + M \rightarrow N_2(A) + M$

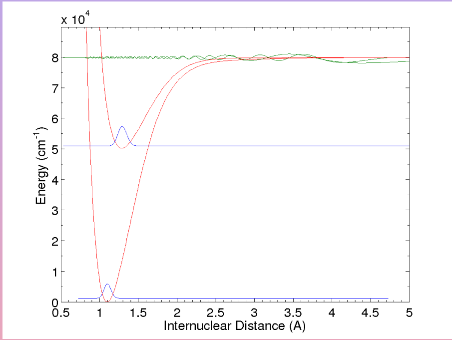

Potential curves and first and last vibrational levels for $N_2(X)$ and $N_2(A)$

Towards an Adequate Accounting of Excited Levels and V–E Rates

- V–E tansitions presented as:
- $N_2(v) + M \rightarrow N_2(A) + M$
- Which means:
- $N_2(X, v = i) + M \rightarrow N_2(A, v = f) + M$

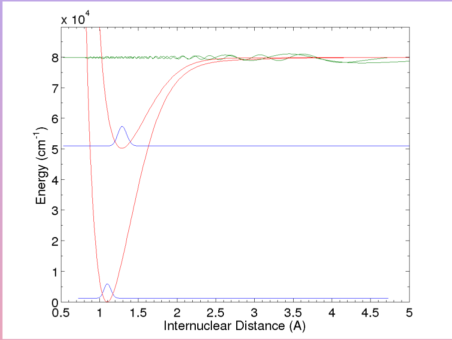

Potential curves and first and last vibrational levels for $N_2(X)$ and $N_2(A)$

Towards an Adequate Accounting of Excited Levels and V–E Rates

- V–E tansitions presented as:
- $N_2(v) + M \rightarrow N_2(A) + M$
- Which means:
- $N_2(X, v = i) + M \rightarrow N_2(A, v = f) + M$
- We replace them by:
- $N_2(X, v_i) + M \rightarrow N_2(X, v_f) + M$
- $N_2(X, v_i) + M \rightarrow N_2(A, v_f) + M$
- $N_2(A, v_i) + M \rightarrow N_2(A, v_f) + M$

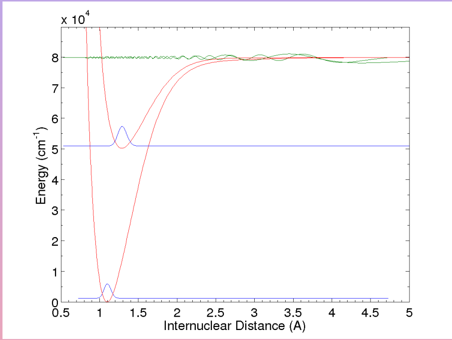

Potential curves and first and last vibrational levels for $N_2(X)$ and $N_2(A)$

0D calculation in the conditions of Fire II

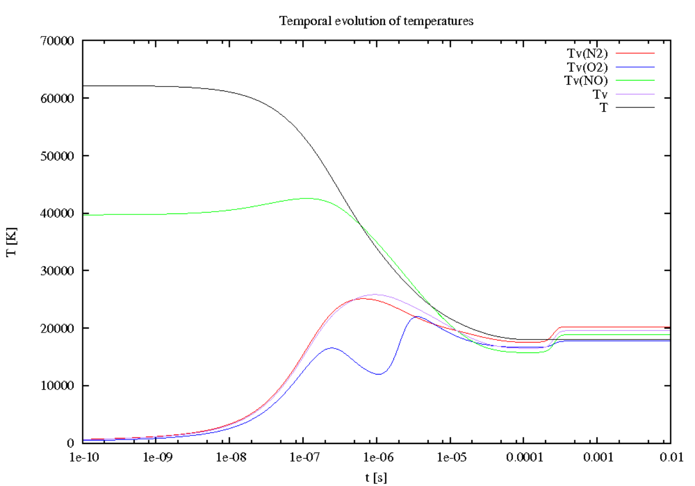

Post-shock average vibrational energies of N_2, O_2 and NO

CFD with Coupled Multiquantum State-to-State Models

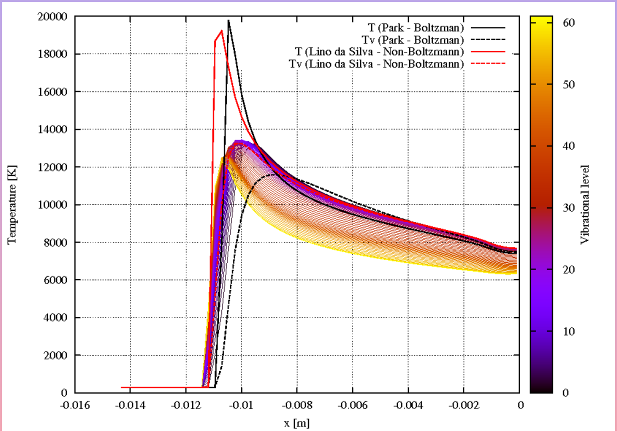

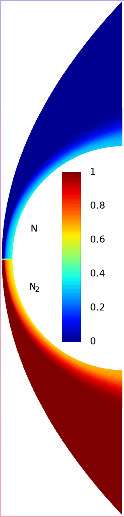

Post-shock excitation of the vibrational levels of N_2, using an N_2–N_2 (FHO, Lino da Silva) and N_2–N (QCT, Esposito) multiquantum kinetic dataset

Conclusions

- The FHO model provides a flexible, yet accurate numerical tool for the production of multiquantum V–T, V–V–T, and V–D rate databases for diatom-diatom collisions.
- A full repulsive 3D FHO approach, including the effects of rotation exists (Macheret& Adamovich) but it is preferred to keep the 1D approach with steric factors, as we can account for repulsive-attractive Morse interactions. Need to carefully tailor the numerical simulation (underflows/overflows) and to select adequate vibrational energies manifolds.
- The diatom-diatom collision databases produced using the FHO model pass all the validation tests (physical consistency, thermodynamic equilibrium consistency, reproduction of available experimental and numerical state-to-state rates from sophisticated models), and provide reliable datasets which will help bridging the transition to full 3D trajectory methods over surface potentials.

Conclusions

- The FHO model provides a flexible, yet accurate numerical tool for the production of multiquantum V–T, V–V–T, and V–D rate databases for diatom-diatom collisions.
- A full repulsive 3D FHO approach, including the effects of rotation exists (Macheret& Adamovich) but it is preferred to keep the 1D approach with steric factors, as we can account for repulsive-attractive Morse interactions. Need to carefully tailor the numerical simulation (underflows/overflows) and to select adequate vibrational energies manifolds.
- The diatom-diatom collision databases produced using the FHO model pass all the validation tests (physical consistency, thermodynamic equilibrium consistency, reproduction of available experimental and numerical state-to-state rates from sophisticated models), and provide reliable datasets which will help bridging the transition to full 3D trajectory methods over surface potentials.

Conclusions

- The FHO model provides a flexible, yet accurate numerical tool for the production of multiquantum V–T, V–V–T, and V–D rate databases for diatom-diatom collisions.
- A full repulsive 3D FHO approach, including the effects of rotation exists (Macheret& Adamovich) but it is preferred to keep the 1D approach with steric factors, as we can account for repulsive-attractive Morse interactions. Need to carefully tailor the numerical simulation (underflows/overflows) and to select adequate vibrational energies manifolds.
- The diatom-diatom collision databases produced using the FHO model pass all the validation tests (physical consistency, thermodynamic equilibrium consistency, reproduction of available experimental and numerical state-to-state rates from sophisticated models), and provide reliable datasets which will help bridging the transition to full 3D trajectory methods over surface potentials.